MOLECULAR AND CELLULAR BIOLOGY, Feb. 2007, p. 1380–1393 Vol. 27, No. 4
0270-7306/07/$08.00+0 doi:10.1128/MCB.01608-06

Asef2 Functions as a Cdc42 Exchange Factor and Is Stimulated by the Release of an Autoinhibitory Module from a Concealed C-Terminal Activation Element[▽]

Michael J. Hamann, Casey M. Lubking, Doris N. Luchini, and Daniel D. Billadeau*

Division of Oncology Research, Mayo Clinic College of Medicine, Rochester, Minnesota 55905

Received 28 August 2006/Returned for modification 17 October 2006/Accepted 27 November 2006

Asef (herein called Asef1) was identified as a Rac1-specific exchange factor stimulated by adenomatous polyposis coli (APC), contributing to colorectal cancer cell metastasis. We investigated Asef2, an Asef1 homologue having a similar N-terminal APC binding region (ABR) and Src-homology 3 (SH3) domain. Contrary to previous reports, we found that Asef1 and Asef2 exchange activity is Cdc42 specific. Moreover, the ABR of Asef2 did not function independently but acted in tandem with the SH3 domain to bind APC. The ABRSH3 also bound the C-terminal tail of Asef2, allowing it to function as an autoinhibitory module within the protein. Deletion of the C-terminal tail did not constitutively activate Asef2 as predicted; rather, a conserved C-terminal segment was required for augmented Cdc42 GDP/GTP exchange. Thus, Asef2 activation involves APC releasing the ABRSH3 from the C-terminal tail, resulting in Cdc42 exchange. These results highlight a novel exchange factor regulatory mechanism and establish Asef1 and Asef2 as Cdc42 exchange factors, providing a more appropriate context for understanding the contribution of APC in establishing cell polarity and migration.

Rho family guanine nucleotide exchange factors (GEFs) are essential links between extracellular signaling events and the activation of Rho family GTPases, acting as the direct facilitators of GDP displacement in these molecular switches. The GTP-loaded and activated Rho family GTPases, such as RhoA, Rac1, and Cdc42, have classically been appreciated for their effects on cytoskeletal reorganization and the establishment of cellular polarity (6, 11) but also are known to induce proliferative responses through the binding and activation of proteins such as p21-activated kinase (PAK) (24) and Rho-associated kinase (33, 35). Despite the potential for direct, unregulated cellular proliferation and metastasis through constitutive activation of Rho family GTPases, activating mutations similar to those established for Ras have not been discovered in human cancers (25). Therefore, Rho family GEFs are frequently investigated in terms of their potential as oncogenic triggers, since they are the first upstream activators of Rho-GTPases and potentially misregulate GTPases when overexpressed or mutated to constitutively active forms (5, 15).

The identification and initial characterization of Asef stand out as a conspicuous example of GEF misregulation in tumor cells (22). Asef (APC [adenomatous polyposis coli]-stimulated exchange factor, hereafter referred to as Asef1) was first identified through a yeast two-hybrid screen using the APC armadillo repeat region (APC^{ARM}) as bait. The APC^{ARM} is an important segment of APC and is retained in APC truncation mutations found in colorectal cancers and familial adenomatous polyposis (4, 16). Although its exact function remains elusive, the APC^{ARM} interaction localized to an APC binding region (ABR) within Asef1, a region lying immediately N-terminal to the protein's Src-homology 3 (SH3) domain. The most profound outcome of the APC-Asef1 interaction is that it stimulates Asef1 GEF activity, leading to Rac1 activation, lamellipod formation, and increased cell migration. Additionally, cells coinfected with full-length Asef1 and the APC^{ARM} migrate more rapidly than cells coinfected with Asef1 and full-length APC, suggesting that Asef1 is inducibly activated by the APC^{ARM} (21). It has therefore been suggested that the truncated forms of APC often found in colorectal cancer and familial adenomatous polyposis are not only devastating due to unregulated cellular β-catenin accumulation but may also enhance cellular metastasis due to constitutive Asef1 activation (8, 13, 22).

Despite the implications that truncated APC may directly impact cytoskeletal dynamics through Rho family GEFs, little has been done to further investigate its unique mode of GEF activation. In order to gain a more complete understanding on how APC impacts cytoskeletal events, we have characterized Asef2, a close homologue of Asef1. While Asef2 GEF activity can be stimulated by an interaction with the APC^{ARM}, our findings demonstrate that Asef1 and Asef2 are in fact Cdc42-specific exchange factors and do not act on Rac1. Moreover, in contrast to Asef1, APC binding to Asef2 is not only mediated by the ABR but also relies mostly upon the adjacent SH3 domain. The tandem ABRSH3 functions as an autoinhibitory module within the protein and binds to the C-terminal region of the protein lying after the canonical Dbl-homology (DH) and pleckstrin homology (PH) domains. Surprisingly, the C-terminal tail of Asef2 not only provides a binding site for the autoinhibitory ABRSH3 but is also required for maximal exchange activity toward Cdc42, with deletion of as little as the last 32 amino acids completely disrupting activity. Therefore, we believe that the primary function of the ABRSH3 is to

* Corresponding author. Mailing address: Mayo Clinic, Division of Oncology Research, 200 First Street SW, Rochester, MN 55905. Phone: (507) 266-4334. Fax: (507) 266-5146. E-mail: billadeau.daniel@mayo.edu.

▽ Published ahead of print on 4 December 2006.

sequester a C-terminal activation element and prevent the tail from participating in Cdc42 GDP/GTP exchange, identifying a novel mode of GEF regulation.

MATERIALS AND METHODS

Reagents and plasmids. All reagents were from Sigma unless specified otherwise. Rabbit antiserum to Asef2 was generated using a peptide corresponding to amino acids 215 to 234 conjugated to keyhole limpet hemocyanin. APC antibody (clone ALI 12-28) was purchased from Upstate Biotechnology. Anti-Cdc42 (clone 44) was purchased from BD Transduction Labs, anti-Rac1 (clone 23A8) was purchased from Upstate, and anti-RhoA (clone 1C1) was purchased from Novus Biologicals. Anti-maltose binding protein (MBP), a purified rabbit polyclonal antibody, was purchased from Immunology Consultants Laboratory, Inc., and anti-green fluorescent protein (GFP) goat polyclonal was from Santa Cruz Biotechnologies. The EE monoclonal antibody to the epitope MEEEEYMPMEA was purified from ascites fluid.

Asef1 (GenBank accession no. AB042199) and Asef2 (AK055770) expression vectors were generated from a cDNA library using oligonucleotides to amplify the open reading frame. N-terminal and C-terminal truncations were amplified from the full-length Asef2 and Asef1 cDNA with appropriate primers. The ABR deletion mutant (ΔABR) was generated using a Stratagene Quikchange Site-Directed Mutagenesis kit. All resulting products were cloned into mammalian expression vectors that incorporated an N-terminal FLAG tag and vectors for generating both untagged and an N-terminal FLAG-hexahistidine (Flag-His)-tagged baculovirus. The sequence corresponding to the Asef1 and Asef2 ABR, SH3, ABRSH3 (see Fig. 4D for amino acids in the coding region), the Asef2 DH-PH (corresponding to amino acids 233 to 561), and the Asef2 C-terminal tail fragment (corresponding to amino acids 561 to 652) were amplified and cloned into pGEX-KG or pMAL-2c (NEB, Boston, MA) to generate either glutathione-*S*-transferase (GST) or MBP fusion proteins. The Asef2 C-terminal tail fragment (amino acids 561 to 652) was also generated as a C-terminal-tagged yellow fluorescent protein (YFP) expression construct. A cDNA fragment containing the APC^{ARM} (coding for amino acids 205 to 885) was amplified from pancreatic tumor cell line cDNA. The product was cloned into a mammalian expression vector containing an N-terminal EE tag, a vector providing a C-terminal YFP tag, and a vector for generating baculovirus capable of expressing an N-terminal MBP fusion protein. A construct expressing a Flag-tagged version of the oncogenic form of Vav1 (ΔCH) was described previously (15). The sequence corresponding to the oncogenic fragment of Lbc has been previously reported and was expressed using vaccinia virus (38). Finally, cDNA fragments encoding the Rho family GTPases were subcloned from cDNAs into baculovirus vectors to generate Flag-His-tagged proteins. Constructs for expressing short hairpin RNAs (shRNAs) to target Asef2 were generated as described previously (18) using the 19-nucleotide sequence 5′-GATGGGAATGGAAATTTCA-3′. Rac1 and Cdc42 shRNAs have been described previously (29).

Cell culture and transfection. HeLa, BxPc3, and Panc04-03 cells were grown in RPMI 1640 medium supplemented with 5% bovine calf serum and 5% fetal bovine serum (FBS), and 4 mM L-glutamine. SW480 cells were grown in Dulbecco's modified Eagle's medium supplemented with 5% bovine calf serum, 5% FBS, and 4 mM L-glutamine. All cell lines were grown at 37°C and 5% CO_2. HeLa, BxPc3, and Panc04-03 cells were transfected via electroporation (350 V for HeLa and 375 V for BxPc3 and Panc04-03 cells; 0.01-s pulse). Typically, 5 to 10 μg of plasmid DNA was used per 3×10^6 HeLa cells or 40 μg of plasmid DNA per 10×10^6 BxPc3 or Panc04-03 cells for each electroporation. After transfection, cells were either allowed to express proteins for 18 h or suppress endogenous proteins for 48 to 72 h prior to experiments. The transfection efficiency of all cell line cells was typically greater than 85%. Sf9 cells were grown at 27°C in Grace's insect cell media supplemented with 10% FBS.

Fusion protein purification. Full-length and truncated versions of Flag-His-tagged and untagged Asef2, an MBP fusion of the APC^{ARM}, and Flag-His-tagged Rho family GTPases were expressed in Sf9 cells using recombinant baculovirus according to the manufacturer's procedures (Invitrogen). Proteins were expressed 72 h postinfection. All the various Flag-His-tagged Asef fusion proteins were purified under the same conditions. Sf9 cells were lysed with 20 mM Tris, pH 8.0, 150 mM NaCl, 1 mM phenylmethylsulfonyl fluoride (PMSF), 10 μg/ml leupeptin, and 5 μg/ml aprotinin; cells were centrifuged, and the clarified supernatant was rotated with Probond resin (Invitrogen) for 20 min at 4°C. Following two washes with Tris-buffered saline (TBS; 20 mM Tris, pH 8.0, 150 mM NaCl) containing 20 mM imidazole, the fusion proteins were eluted with TBS containing 300 mM imidazole. Sf9 cells expressing MBP fusions were lysed in the same lysis buffer. The clarified lysate was applied to amylose resin and incubated for 30 min at 4°C. The resin was extensively washed with TBS and eluted in TBS containing 15 mM maltose.

Flag-His-tagged versions of the lipid-modified and unmodified forms of the Rho family GTPases were isolated from insect cells as previously described (40). Briefly, lysates were prepared using a lysis buffer containing 10 mM Tris, pH 7.4, and 10 mM $MgCl_2$ with protease inhibitors. The clarified lysate was added to Probond resin to purify unmodified GTPases. The pelleted material was resuspended in lysis buffer and recentrifuged. After the buffer was removed, the pellet was resuspended in extraction buffer containing 20 mM Tris, pH 8.0, 5 mM $MgCl_2$, 1 mM EDTA, and 0.6% CHAPS (3-[(3-cholamidopropyl)-dimethylammonio]-1-propanesulfonate), and the insoluble materials were removed by centrifugation. The clarified supernatant was used to purify lipid-modified GTPases. After incubation with Probond, both the lipid-modified and the unmodified GTPases were washed with extraction buffer, followed by a wash with TBS containing 20 mM imidazole, and were eluted in TBS containing 300 mM imidazole.

Bacterially expressed GST fusion proteins were purified essentially as described previously (37). Proteins were expressed in *Escherichia coli* strain BL21(DE3) by growing bacteria at 37°C in LB medium supplemented with 100 μg/ml ampicillin and by induction with 40 μM isopropyl-β-D-thiogalactopyranoside after cultures reached an optical density at 600 nm of 0.5. The bacteria were then grown overnight at 18°C. After the bacterial cells were pelleted by centrifugation, the pellet was resuspended and sonicated in phosphate-buffered saline (PBS) supplemented with 1% Triton X-100, 0.03% sodium dodecyl sulfate (SDS), 10 mM dithiothreitol (DTT), 1 mM PMSF, 10 μg/ml leupeptin, and 5 μg/ml aprotinin. The clarified lysate was then rotated with glutathione (GSH)-agarose slurry for 20 min at 4°C. After the incubation, the agarose was spun down and washed with PBS containing 1% Triton X-100 and 0.1% β-mercaptoethanol, followed by washing with PBS containing 0.1% Triton X-100 and 0.1% β-mercaptoethanol. GST fusion proteins were eluted in the final wash buffer supplemented with 20 mM glutathione and then dialyzed overnight. MBP fusion proteins were expressed in the same manner as GST fusion proteins; however, pellets were lysed in 20 mM Tris, pH 8.0, 150 mM NaCl, 1 mM PMSF, 10 μg/ml leupeptin, and 5 μg/ml aprotinin. The lysis buffer was used for washing the amylose resin, and the bound protein was eluted in buffer containing 10 mM maltose. Protein concentrations were determined using Bradford assays or gel densitometry by comparing the band corresponding to a purified protein to dilutions of bovine serum albumin run concurrently on an SDS-polyacrylamide gel electrophoresis (PAGE) gel and stained with Coomassie blue.

Guanine nucleotide exchange assays. Exchange assays were conducted essentially as described elsewhere (22, 27, 28). For each individual assay, GTPases were loaded with [^{3}H]GDP in a buffer containing 20 mM Tris, pH 8.0, 1 mM EDTA, 1 mM DTT, and 0.2 μM [^{3}H]GDP for 20 min at 37°C. Following the incubation, 200 mM $MgCl_2$ was added to a final concentration of 5 mM, and the mixture was incubated at room temperature for 5 min. For exchange reactions, the GTPases were diluted threefold in buffer containing 20 mM Tris, pH 8.0, 150 mM NaCl, and the appropriate amount of exchange factor. The final concentrations of GTPase and exchange factor were typically 250 and 20 nM, respectively, unless otherwise stated. The exchange reaction was started by adding a 250-fold excess of unlabeled GTP, and aliquots were removed at time points identified in the figure legends, diluted in 1 ml of stop buffer (20 mM Tris, pH 8.0, 50 mM NaCl, and 25 mM $MgCl_2$), and passed through nitrocellulose filters. The filters were washed with 4 ml of stop buffer and dried, and the bound [^{3}H]GDP was counted via liquid scintillation. All experiments involving incubation of Flag-His-Asef2 or -Asef2 truncation mutants with a second fusion protein were conducted in 20 mM Tris, pH 8.0, and 150 mM NaCl for 30 min at room temperature prior to being added to [^{3}H]GDP-loaded Cdc42.

GTPase activation assay. The GTP-bound form of endogenous Cdc42 and Rac1 was detected using the standard GST-PAK affinity precipitation assay with some modifications (2). Briefly, 20 μg of a GST fusion protein containing the Cdc42/Rac interactive binding (CRIB) region of PAK was bound to GSH agarose in PAK-CRIB binding buffer (20 mM Tris, pH 8.0, 30 mM NaCl, 25 mM $MgCl_2$, 0.5% NP-40, 1 mM DTT, 1 mM $NaVO_4$, 1 mM PMSF, 10 μg/ml leupeptin, 5 μg/ml aprotinin) at 4°C for 30 min, followed by one wash with PAK-CRIB binding buffer. Transfected cells grown in serum-containing medium were rested for 4 h in serum-free medium prior to the assay, washed once on ice with ice-cold PBS, and lysed with activation assay lysis buffer (25 mM Tris, 50 mM NaCl, 5% glycerol, 0.5% NP-40, 1 mM DTT, 1 mM $NaVO_4$, 1 mM PMSF, 10 μg/ml leupeptin, 5 μg/ml aprotinin). Cells were collected and lysed by scraping the plate, the lysate was clarified by centrifugation at $12,000 \times g$ for 1 min at 4°C, and the resulting supernatant was applied to the GST-PAK-CRIB/GSH agarose complex. The lysate and beads were rotated for 15 min at 4°C before being washed once with PAK-CRIB binding buffer. RhoA activation was detected in an

analogous manner except that a GST fusion protein of the rhotekin Rho binding domain was used to precipitate active RhoA. Samples were analyzed by immunoblotting.

GST fusion protein coprecipitation and immunoprecipitation assays. Twenty micrograms of GST fusion protein was incubated with GSH-agarose slurry in Nonidet-P40 (NP-40) lysis buffer (20 mM HEPES, pH 7.9, 100 mM NaCl, 5 mM EDTA, 0.5 mM CaCl, 1% NP-40, 1 mM PMSF, 10 μg/ml leupeptin, 5 μg/ml aprotinin) for 30 min at 4°C, followed by one wash with the same buffer. Cells were washed one time with ice-cold PBS and lysed with lysis buffer and scraping, and the resulting suspension was clarified at 12,000 × *g* for 5 min at 4°C. Approximately 1 mg of clarified lysate was incubated with the GST fusion protein-GSH agarose complex at 4°C for 45 min and washed twice with NP-40 lysis buffer before samples were prepared for analysis by SDS-PAGE (18). Binding experiments using purified MBP or Flag-His-tagged proteins were conducted using the same procedure, except that recombinant protein (usually 1 μg of MBP and 0.25 μg of Flag-His protein) was added to 1 ml of NP-40 lysis buffer and used directly in the assay.

Coimmunoprecipitation experiments were conducted using monoclonal or rabbit antibodies bound to either anti-mouse immunoglobulin G (IgG) agarose or protein A Sephadex (respectively) in 25 mM HEPES, pH 7.4, 150 mM NaCl, 5 mM EDTA, 0.5% $CaCl_2$, 0.2% NP-40, 0.2% Tween-20, 10% glycerol, 1 mM PMSF, 10 μg/ml leupeptin, and 5 μg/ml aprotinin. Cells were lysed in the same buffer, and clarified supernatant (containing about 1 mg of total protein) was rotated with the antibody-agarose complex for 1 h at 4°C. The resulting precipitate was washed once with buffer and prepared for analysis by SDS-PAGE.

Immunofluorescence. BxPc3 cells, a pancreatic ductal tumor cell line, were used to detect filopodia generated by Asef2, as the filopodia were robust and easily visualized. For imaging, cells grown on coverslips were washed once with PBS and fixed using PBS containing 4% paraformaldehyde. After incubation for 10 min at room temperature, the coverslips were washed once with PBS and permeabilized with 0.1% Triton X-100 for 5 min at room temperature. The coverslips were blocked for 30 min in PBS containing 5% goat serum, 1% glycerol, 0.1% fish skin gelatin, 0.1% bovine serum albumin, and 0.04% sodium azide at room temperature and incubated with the appropriate primary and secondary antibodies in blocking buffer for 1 h, with four PBS washes in between incubation with each antibody. Actin was visualized with rhodamine phalloidin (Molecular Probes). Slips were mounted with a layer of AntiFade and visualized with an Axioplan (Zeiss) microscope.

Migration assays. Panc04-03 cells were transfected with a control vector (pCMS3.H1P) and shRNA suppression vectors for either Asef2 or Cdc42. After 72 h, the cells were dissociated from a tissue culture dish with cell dissociation solution (Sigma), and 2.5×10^4 cells were added to the upper surface of a fibronectin-treated (10 μg/ml in PBS for 12 h) Transwell chamber (6.5-mm diameter and 8.0-μm pores; Corning). Cells were allowed to migrate for 18 h before the cells remaining on the upper side of the membrane were removed and the cells on the lower portion of the membrane were fixed using PBS containing 4% paraformaldehyde. The pCMS3 shRNA vectors contain a separate transcriptional cassette for expression of GFP, and only GFP-positive cells were counted using fluorescent confocal microscopy.

RESULTS

Asef2 homology and GTPase substrate. There are 69 Rho family GEFs in the human genome, and aside from the canonical DH-PH cassette found in virtually all of them, many of these GEFs, including Vav, faciogenital dysplasia (FGD) protein, and Sos form clusters or families that are highly similar based on overall domain architecture (34). The Asef family of proteins circumscribes a series of GEFs that include Asef1, Asef2, and collybistin I (also known as hPEM-2 and ArhGef9) (23, 30), all of which contain an N-terminal SH3 domain followed by the DH-PH cassette and no other obvious domain structures (Fig. 1A). Asef1 and Asef2 contain an additional N-terminal sequence, part of which was identified in Asef1 as an ABR, lying between amino acids 73 and 126. A similar region is present in Asef2, between amino acids 90 and 152, which suggested that Asef2 could be activated by APC in a manner comparable to Asef1. The fact that many reported splice variants of Asef1 and Asef2 retain the central ABR, SH3, DH, and PH domain architecture further supports the idea that these are key functional elements within the proteins (Fig. 1B). Although it remains to be seen if Asef1 and Asef2 are entirely redundant functional homologues of each other, independent regulation of the two GEFs by APC may simply be reflected in the different tissue distributions of the mRNA transcripts detected using Northern blots and gene-specific probes (Fig. 1C).

Initial experiments were aimed at determining which Rho GTPase was the appropriate substrate for Asef2. GST fusions of dominant-negative versions of Rac1, Rac3, RhoA, and Cdc42 were provided as bait in an in vitro binding assay, where a Flag-tagged N-terminal truncation mutant of Asef2 (Δ204) was expressed in cells. An N-terminal truncation mutant of Asef2 was used in the initial screening assay since GEFs are frequently self-regulated through discreet, autoinhibitory segments, potentially preventing access and binding of the GTPase to the GEF's catalytic DH and PH domains (1, 3, 36). Initial reports on Asef1 suggested that deleting the ABR from the protein was sufficient to constitutively activate the GEF; however, we chose to eliminate almost all of the N-terminal sequence adjacent to the DH-PH domains, including the entire SH3 domain. In agreement with previous observations, we found that Asef2 bound to Rac1. The binding was highly specific to Rac1, and a fusion protein of Rac3 failed to precipitate Asef2 (Fig. 2A), despite having greater than 90% sequence similarity.

While the binding assay provided evidence that Asef2 was likely to be a Rac1-specific GEF, these assays do not always reflect which GTPase can be GTP-loaded by a particular GEF. Therefore Rac1, RhoA, and Cdc42 were used in an in vitro exchange assay to test Asef2 for activity toward Rac1. Furthermore, the GTPases used in the assay were purified from Sf9 cells as lipid-modified proteins, as some Rho-GEFs, such as FGD1, have been reported to require lipid-modified GTPase substrates in exchange reactions (41). The Δ204 mutant of Asef2 was expressed and purified as recombinant fusion proteins in Sf9 cells (Fig. 2B). Additionally, a corresponding truncation mutant was produced for Asef1 (Δ180) and used as a positive control in the assay. Surprisingly, both the Asef2 Δ204 and the Asef1 Δ180 truncation mutants showed no activity toward Rac1 but instead exchanged Cdc42. The exchange activity of Asef2 was only detected with the lipid-modified form of Cdc42 (Fig. 2C), demonstrating a substrate preference similar to that reported for FGD1. The recombinant Rac1 used in the assay was functional, since a MBP fusion of the Vav1 DH-PH and cysteine-rich region rapidly exchanged the protein in vitro (Fig. 2D).

The activity of Asef2 toward Cdc42 was confirmed using affinity precipitation assays to detect increases in GTP-loaded Rac1, RhoA, and Cdc42 from cells expressing either a full-length version or the Δ204 mutant of Asef2. Oncogenic fragments of Vav1 and Lbc were used as positive controls for Rac1 and RhoA, respectively, in this experiment, and clearly demonstrate that Asef2 activity is Cdc42 specific (Fig. 2E). Furthermore, the activity detected in the assay was contingent upon the Δ204 mutant's acting as a functional GEF, since mutations which are known to inactivate either the DH domain (L259Q) or the PH domain (W552L) of Rho family GEFs (34) prevented Asef2-catalyzed activation of Cdc42 (Fig. 2F).

It was previously reported that the ABR was the essential

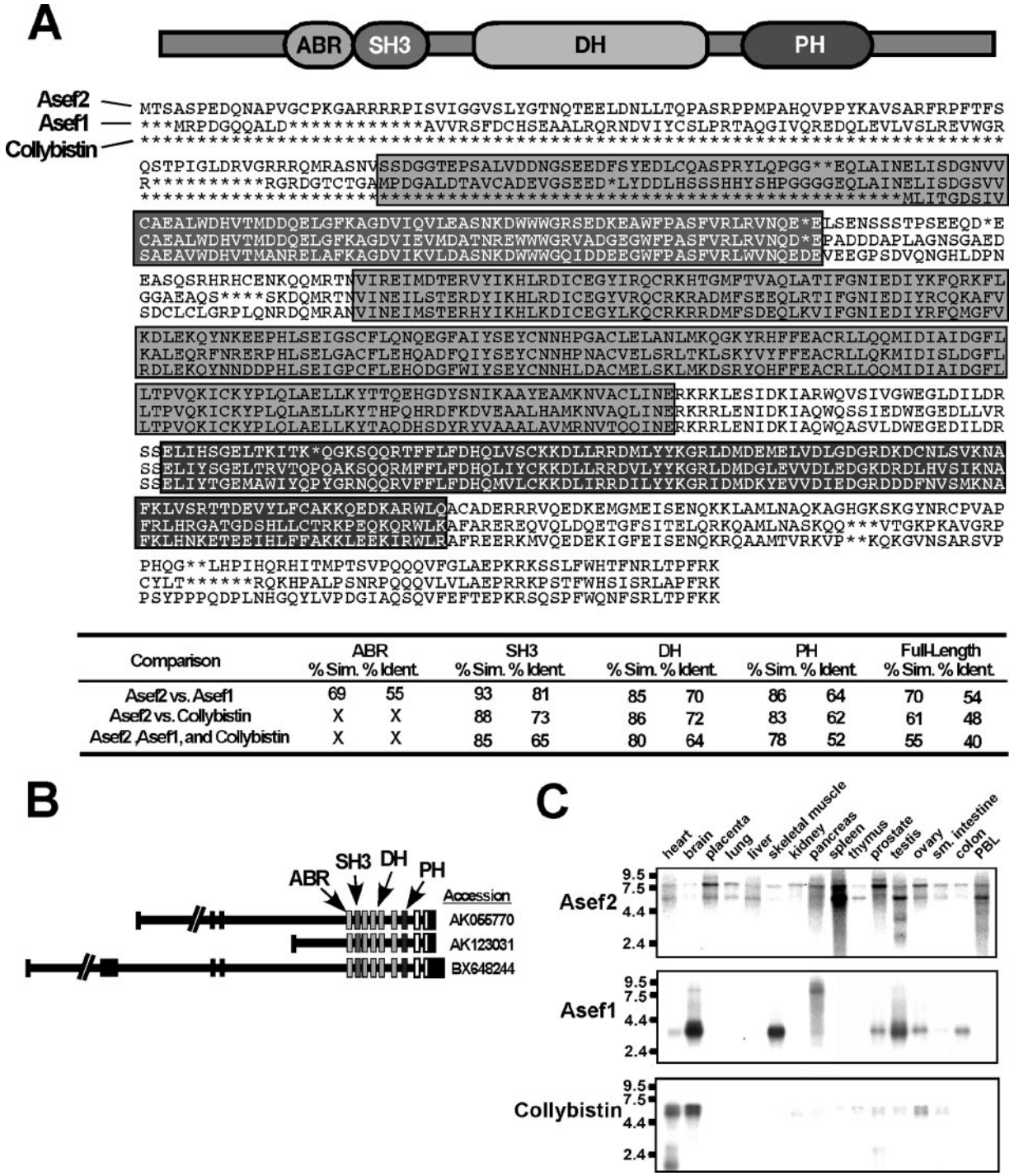

Comparison	ABR % Sim.	ABR % Ident.	SH3 % Sim.	SH3 % Ident.	DH % Sim.	DH % Ident.	PH % Sim.	PH % Ident.	Full-Length % Sim.	Full-Length % Ident.
Asef2 vs. Asef1	69	55	93	81	85	70	86	64	70	54
Asef2 vs. Collybistin	X	X	88	73	86	72	83	62	61	48
Asef2, Asef1, and Collybistin	X	X	85	65	80	64	78	52	55	40

FIG. 1. Asef2 homology and tissue expression. (A) Sequences corresponding to Asef2, Asef1, and collybistin I (GenBank accession NM_015185) were aligned using CLUSTALW. The sequences corresponding to the ABR, SH3, DH, and PH domains are gray scaled according to the diagram of Asef2 provided at the top of the alignment. The table at the bottom of the alignment provides the percent homology of the different domains within the three proteins. (B) Exons coding for the ABR, SH3, DH, and PH domains are conserved among multiple Asef2 transcript variants. Exons corresponding to the Asef2 sequence used in this study (AK055770) have been gray scaled for the indicated domains according the diagram provided at the top of panel A. GenBank accession numbers AK123031 and BX648244 represent Asef2 variants containing the same basic domain structures. (C) Asef2, Asef1, and collybistin have different tissue expression profiles. Northern blot analysis was performed using ^{32}P-labeled antisense oligonucleotide probes for Asef2 (nucleotides 1163–1908), Asef1 (nucleotides 451 to 1303), and collybistin I (nucleotides 832 to 2347) and hybridized to a commercially available multiple tissue array (BD Biosciences Clontech) using the manufacturer's protocols. Collybistin I mRNA is primarily expressed in the brain, in agreement with previous observations (30). Sim, similarity; Ident, identity.

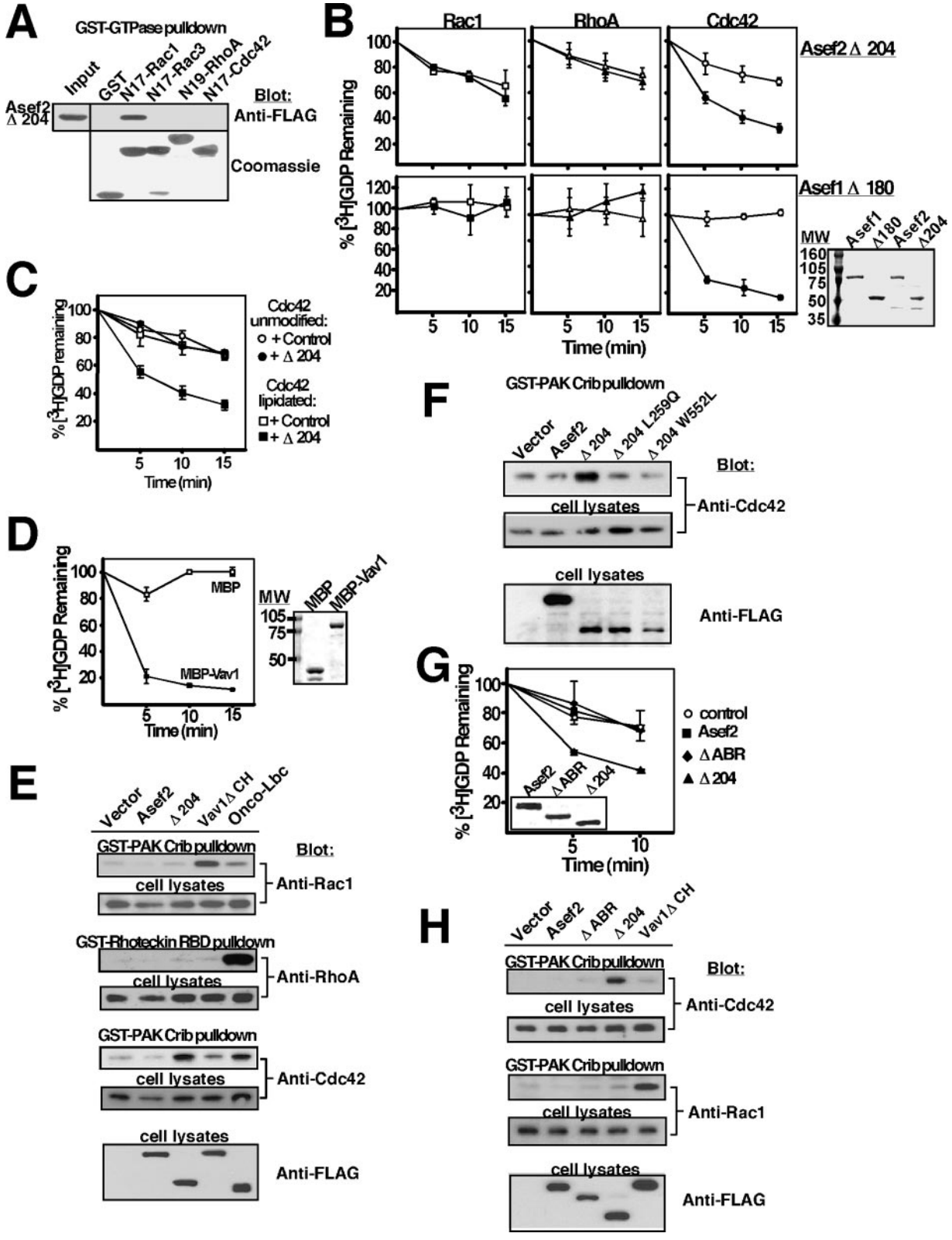

FIG. 2. Asef2 is an exchange factor for Cdc42. (A) Lysates from BxPc3 cells expressing a Flag-tagged, N-terminal truncation mutant of Asef2 (Δ204) were incubated with GST fusion proteins of the indicated dominant-negative Rho family GTPases bound to GSH agarose. Coprecipitating Asef2 was detected by immunoblotting with an anti-Flag antibody. (B) In vitro exchange activity of the Flag-His-tagged Asef2 Δ204 and the Asef1 Δ180 mutants towards [^{3}H]GDP-loaded lipid-modified Rac1, RhoA, and Cdc42. Open symbols indicate a buffer control; closed symbols indicate GTPases incubated with the GEF. Points represent the mean of triplicate samples, and error bars show ± standard deviation. The image of a Coomassie stained SDS-PAGE gel indicates the purity of one μg of Flag-His-tagged full-length Asef1 and Asef2, as well as the N-terminal

regulatory structure within Asef1, required for both APC binding and autoinhibition of Asef1. We made a deletion mutant of this region within Asef2 but found that the Asef2 ΔABR mutant failed to exchange Cdc42 in vitro (Fig. 2G). Furthermore, expression of the ΔABR deletion mutant in HeLa cells failed to increase the amount of precipitated, GTP-loaded Cdc42 in comparison to expression of the Asef2 Δ204 mutant (Fig. 2H). Since only the Δ204 mutant demonstrated a capacity to rapidly exchange Cdc42 in both assays, we concluded that the ΔABR mutation does not completely eliminate Asef2 autoinhibition and that an additional N-terminal region, probably the SH3 domain, was also involved. Notably, Rac1 activation remained unchanged with expression of either the ΔABR or the Δ204 mutant, showing that the Δ204 mutation does not somehow alter the GTPase specificity of Asef2.

We also examined the effect of Asef2 on cell morphology (Fig. 3A), since activation of Rho family GTPases has characteristic influences on actin structures within a cell (6, 31, 32). Cells transfected with either YFP or a YFP-tagged version of full-length Asef2 typically showed a rounded shape with few obvious actin structure formations; however, the Δ204 mutant produced elongated filopodial cellular extensions consistent with Cdc42 activation. The filopodia were less numerous compared to cells expressing the constitutively active Q61L mutant of Cdc42 but were thicker and extended further from the central cell body. Cells expressing the Δ204 mutant of Asef2 bore little resemblance to cells expressing constitutively active Rac1, which produced obvious lamellipodia. Furthermore, filopodia induced by the Δ204 mutant were clearly dependent upon Cdc42, since suppression of Cdc42 had a significantly greater effect on preventing filopodia protrusions in comparison to suppression of Rac1 (Fig. 3B).

Using affinity precipitation assays, we found that suppression of endogenous Asef2 affected the level of activated Cdc42 in Panc04-03 (Fig. 3C), a transfectable pancreatic tumor cell line that expresses a high level of endogenous Asef2. Suppression of Asef2 in these cells led to a corresponding decrease in the amount of active Cdc42, although the total levels of Cdc42 protein remained unchanged. Suppression of Asef2 also led to a decrease in the number of cells that were capable of migrating through the pores of a Transwell chamber, similar to Cdc42 suppression (Fig. 3D). Together, these results support the notion that Cdc42 is an in vivo substrate of Asef2 and that Asef2 contributes to cellular migration.

The SH3 domain of Asef2 contributes to binding of the APC^{ARM}. Given the high degree of sequence similarity between Asef1 and Asef2, we hypothesized that an interaction between APC and Asef2 would essentially reflect the interaction between APC and Asef1. An association between Asef2 and APC was tested using Asef2 and APC-specific antibodies in coimmunoprecipitation experiments (Fig. 4A). APC coprecipitated with Asef2 from SW480 cell lysates, and the interaction was also detected in reciprocal experiments. Furthermore, immunofluorescent staining of Asef2 and APC demonstrates that the proteins colocalized in Panc04-03 cells (Fig. 4B).

To verify that the interaction between the APC^{ARM} and Asef2 involves the ABR, cells were cotransfected with EE-tagged APC^{ARM} along with either FLAG-tagged wild-type Asef2, the ΔABR mutant, or the Δ204 truncation mutant, and associations were detected by coimmunoprecipitation (Fig. 4C). Both wild-type Asef2 and the ΔABR mutant coimmunoprecipitated with the APC^{ARM}, demonstrating that deleting the ABR region was insufficient for eliminating the interaction. Since no interaction was detected with the Δ204 deletion mutant in these experiments, we decided to test whether the Asef2 SH3 domain participated in binding the APC^{ARM} and generated GST fusion proteins containing either the Asef1 or Asef2 ABR, the SH3 domain, and the ABRSH3 in tandem (shown schematically in Fig. 4D). In contrast to the GST-ABR of Asef1, which precipitated an EE-tagged version, the APC^{ARM}, no interaction was detected with the GST-ABR of Asef2 despite the inclusion of 20 extra amino acids C-terminal to the ABR (Fig. 4E). Instead, coprecipitation of the APC^{ARM} only occurred with either the tandem Asef2 ABRSH3 or the SH3 domain alone. The ABRSH3 and SH3 domain from Asef1 likewise coprecipitated the APC^{ARM}, demonstrating that the SH3 domain contributes to stabilizing the APC^{ARM} interaction for both Asef1 and Asef2. Despite a high degree of sequence similarity, the SH3 domain of collybistin was incapable of coprecipitating the APC^{ARM} (data not shown), illustrating the specificity of the APC-Asef interactions. These results provide evidence that the SH3 domain is a required compo-

truncation mutants used in the exchange assay. (C) Lipid-modified and unmodified versions of Cdc42 were purified and used in an exchange assay with the Δ204 mutant. (D) Lipid-modified Rac1 was used in an exchange assay with an MBP fusion protein of the Vav DH-PH region (also containing the cysteine-rich domain). The offset panel indicates the purity of MBP-tagged Vav used in the assay. For both B and C, the points indicate the mean of triplicate samples and error bars ± standard deviation. (E) Lysates from BxPc3 cells expressing FLAG-tagged Asef2, the Δ204 truncation mutant, the ΔCH mutant of Vav1, and the truncated oncogenic form of Lbc were split and precipitated with either the GST-PAK-CRIB fusion protein to detect activated Rac1 and Cdc42 or with the GST-rhoteckin Rho binding domain fusion protein to detect activated RhoA. Activated Rac1, RhoA, and Cdc42 were detected via immunoblotting using the appropriate, specific antibodies. Cell lysates represent 10 μg of total protein and show comparable levels of endogenous Rac1, RhoA, and Cdc42 in each of the pull-downs and equivalent expression of the FLAG-tagged GEF constructs. (F) Lysates from HeLa cells expressing Asef2, the Δ204 mutant, and the Δ204 mutant containing a DH domain-inactivating mutation (L259Q) and a PH domain-inactivating mutation (W552L) were incubated with the GST-PAK-CRIB fusion protein, and the amount of active Cdc42 was detected via immunoblotting. (G) Flag-His-tagged version of the Asef2 ΔABR mutant could not be expressed in Sf9 cells. Therefore, untagged versions of full-length Asef2, the ΔABR, or the Δ204 truncation mutants were expressed, and 150 μg of lysate protein was used in an exchange assay with [^{3}H]GDP Cdc42. All other conditions were identical to the procedure in Materials and Methods. The insert shows the relative expression levels of the proteins in 5 μg of lysate using immunoblotting with an Asef2-specific antibody. Points indicate the mean of triplicate samples and error bars show ± standard deviation. (H) HeLa cells expressing FLAG-tagged Asef2, the ΔABR mutant, the Δ204 mutant, or the ΔCH mutant of Vav1 were lysed; and activated, GTP-loaded Cdc42 and Rac1 were precipitated using the GST-PAK-CRIB fusion protein and detected via immunoblotting using a Cdc42 or Rac1-specific antibody. Cell lysates represent 10 μg of total protein and show comparable levels of endogenous Cdc42, Rac1, and the FLAG-tagged Asef2 constructs. The blots reflect data from two independent experiments.

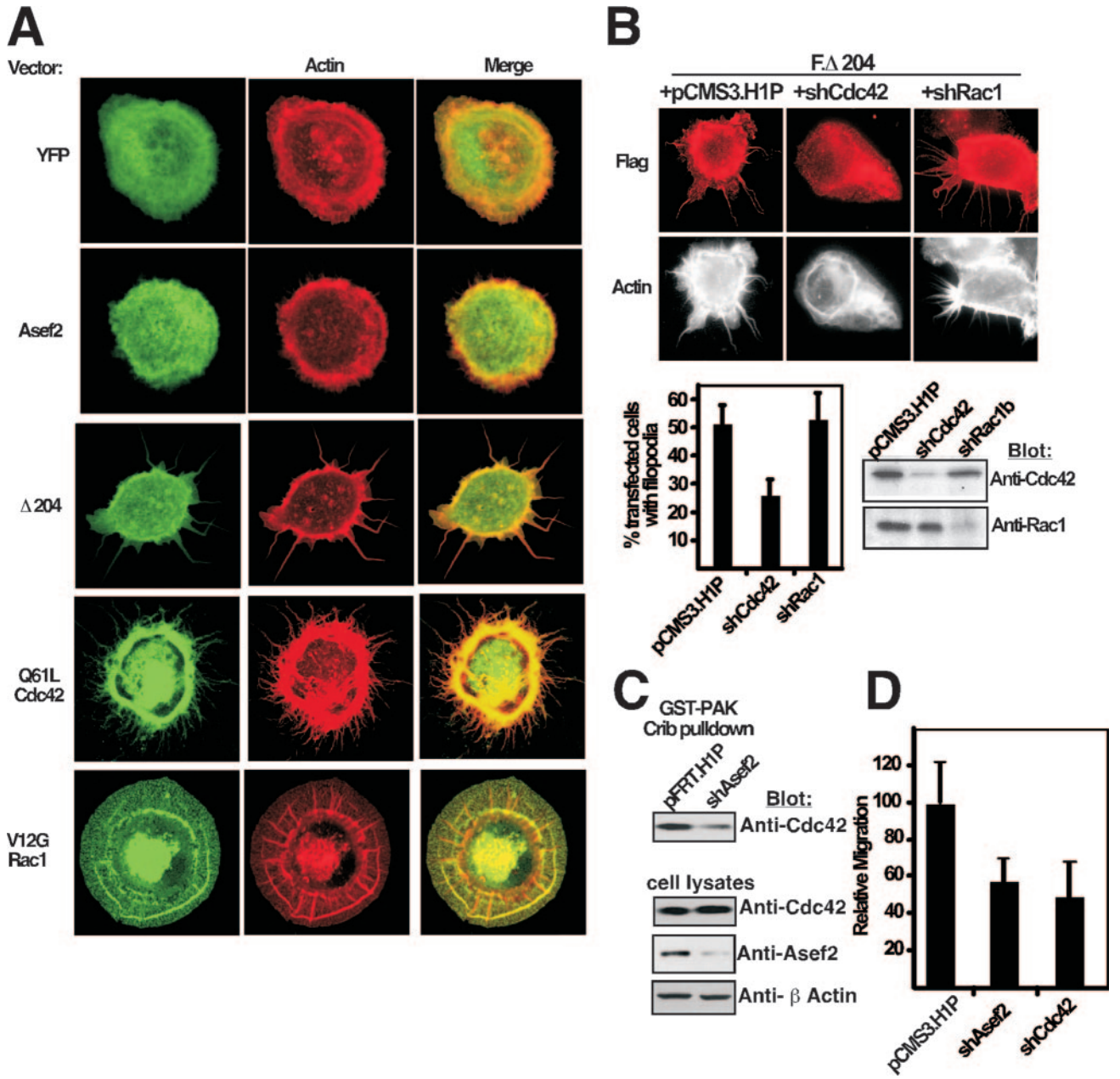

FIG. 3. Asef2 stimulates cellular filopodia through Cdc42 and is important for cell migration. (A) BxPc3 cells expressing YFP-tagged full-length Asef2, the Δ204 mutant, or constitutively active Cdc42 (Q61L) and Rac1 (V12G) were grown for 24 h on coverslips. The cells were fixed and were actin stained with rhodamine-phalloidin. (B) BxPc3 cells were cotransfected with the FLAG-tagged Δ204 mutant expression vector and vectors to generate shRNAs against either Cdc42 or Rac1. Cells were plated on a 60-mm dish with glass coverslips and grown for 48 h before fixing and staining. Cells were scored for the presence or absence of filopodia by an individual who was blinded to the identity of a particular sample. Only cells that were positive for both FLAG staining and GFP expression were counted. The bars on the graph represent the mean results from three different coverslips and error bars represent ± standard deviation. Lysates were prepared from the cells remaining on the 60-mm dish to determine the extent of Cdc42 and Rac1 suppression by immunoblotting (displayed to the right of the graph). Panels above the graph display representative cells expressing both the Flag-tagged Δ204 mutant (shown in red) and GFP. Alexa 350-phalloidin (Molecular Probes) was used for actin staining (shown as black and white images). (C) Panc04-03 cells transfected with a vector expressing shRNAs against Asef2 were used in a pull-down assay with the PAK-CRIB. Protein expression in the cell lysates was detected using 15 μg of total protein and immunoblotting with the indicated antibodies. The blots present representative data from two independent experiments. β-Actin is presented as a loading control. (D) Panc04-03 cells were transfected with a control vector or shRNA vectors against Asef2 or Cdc42 and plated in a Transwell migration chamber as described in Materials and Methods. Data represent the relative migration of Asef2 and Cdc42-suppressed Panc04-03 cells in comparison to control cells, with the bars representing the mean of four separate Transwell chambers ± standard deviation.

nent of the APC^{ARM} recognition site for Asef1 and particularly for Asef2.

The APC^{ARM} stimulates Asef2. The most significant feature of the Asef1-APC^{ARM} interaction was its stimulating effect on Asef1 exchange activity. In order to determine whether Asef2 was also stimulated by APC, we generated an MBP fusion protein of the APC^{ARM} in Sf9 cells (Fig. 5A, blot) for use in exchange assays with Asef2 and Cdc42. While neither the

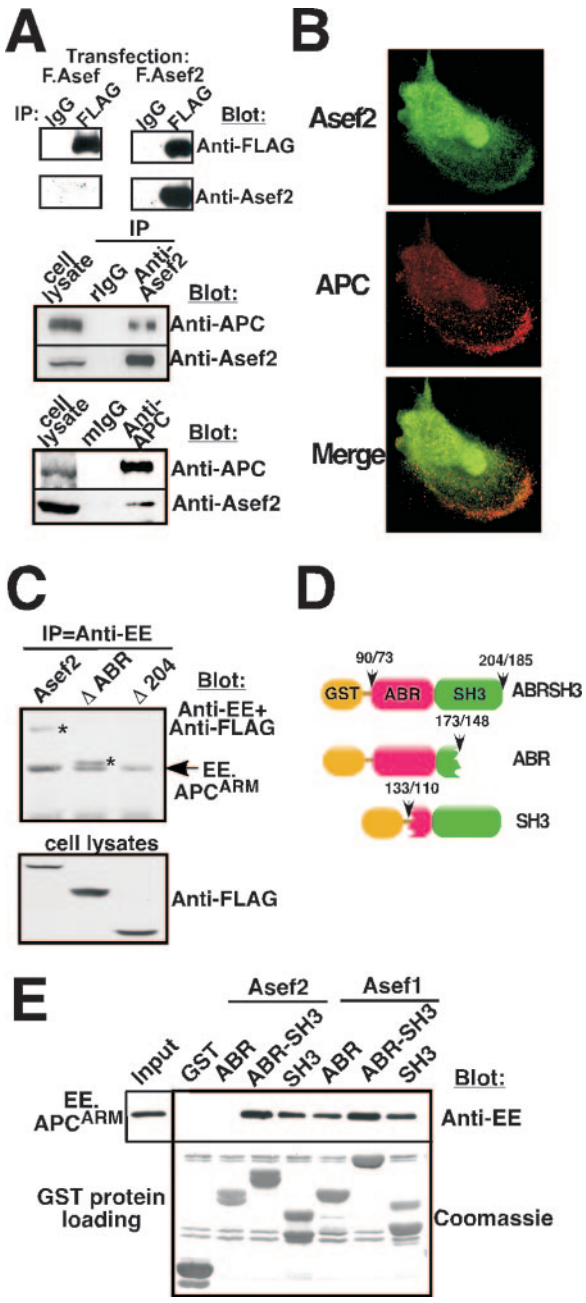

FIG. 4. APC binds Asef2 through the ABRSH3. (A) An Asef2 antibody was used in coimmunoprecipitation experiments. The top portion of the panel indicates that the Asef2 antibody does not cross-react with Asef1. Lysates from HeLa cells expressing full-length FLAG-tagged Asef1 and Asef2 were immunoprecipitated with either mouse IgG or an anti-FLAG antibody and immunoblotted with either an anti-FLAG antibody or an anti-Asef2 antibody. For the coimmunoprecipitation experiments displayed in the lower potion of the figure, lysates from SW480 cells were incubated with either an APC- or Asef2-specific antibody bound to an agarose resin. Coprecipitated Asef2 or APC was detected via immunoblotting. Mouse and rabbit IgGs were used as immunoprecipitation (IP) controls. (B) Endogenous Asef2 and APC were detected in fixed and permeabilized Panc04-03 cells using Asef2 and APC antibodies. Asef2 was detected with a fluorescein isothiocyanate anti-rabbit secondary antibody, while APC was detected with tetramethylrhodamine-conjugated anti-mouse secondary antibody. (C) Lysates from cells coexpressing an EE-tagged version of the APC^{ARM} and either FLAG-tagged full-length Asef2, the ΔABR mutant, or the Δ204 mutant were immunoprecipitated with an anti-EE antibody bound to agarose resin. Coprecipitated FLAG-tagged proteins were detected using immunoblotting. Immunoprecipitated EE-tagged APC^{ARM} is indicated with an arrow, and coprecipitated FLAG-Asef2 and the ΔABR mutant are marked with asterisks. (D) Schematic of the Asef1 and Asef2 ABR, SH3, and ABRSH3 GST fusion proteins designed for coprecipitation experiments. The numbers indicate the first and last amino acids incorporated into the fusion proteins for Asef2 (before slash) and Asef1 (after slash). (E) Lysates from cells expressing EE-tagged APC^{ARM} were incubated with the GST fusion proteins indicated in panel D. Coprecipitated APC^{ARM} was detected using immunoblotting and an anti-EE antibody.

$MBP\text{-}APC^{ARM}$ alone nor Asef2 incubated with MBP augmented exchange activity, an equal-molar concentration of the $MBP\text{-}APC^{ARM}$ stimulated Asef2 activity to a level that was comparable to the Δ204 truncation mutant (Fig. 5A). Likewise, there was an increased amount of active Cdc42 precipitated from HeLa cells coexpressing full-length Asef2 and a YFP-tagged version of the APC^{ARM} in comparison to cells expressing either full-length Asef2 and YFP or the YFP-tagged APC^{ARM} alone (Fig. 5B). The amount of active Cdc42 detected with cells coexpressing Asef2 and the APC^{ARM} was comparable to the Δ204 truncation mutant. Coexpression of Asef2 and the APC^{ARM} did not change Rac1 activity.

Coexpression of $YFP\text{-}APC^{ARM}$ and Asef2 stimulated the formation of filopodia-like projections from the cellular surface (Fig. 5C, bottom frames) and also markedly altered their cellular localization, moving both proteins from a cytosolic distribution to the filopodia structures on the cell perimeter. In comparison, the Δ204 truncation mutant induced filopodia and displayed peripheral localization with coexpression of either YFP or $YFP\text{-}APC^{ARM}$. Furthermore, the $YFP\text{-}APC^{ARM}$ did not display significant accumulation in filopodia, probably because the Δ204 mutant lacks the ABRSH3. Altogether, the results demonstrate that the unique mechanism of Asef activation remains conserved between Asef1 and Asef2, even though both appear to be Cdc42-specific exchange factors.

The ABRSH3 regulates Asef2 activity and binds to the C-terminal tail. Our exchange assays indicated that the ABR was not the sole N-terminal autoinhibitory region within Asef2. Since the ΔABR mutant was an internal deletion mutant, it was necessary to design additional N-terminal truncations that either removed the amino acid sequence before the ABRSH3 (Δ90) or retained only the SH3 domain (Δ140) in order to pinpoint whether an autoinhibitory segment was N-terminal or C-terminal to the ABR (Fig. 6A). Only the Δ204 mutant displayed a clear increase in Cdc42 activation in precipitation assays (Fig. 6B), demonstrating that the SH3 domain retained by the Δ140 mutant was sufficient for inhibiting Asef2 activity. We decided to define how the Asef2 ABR, SH3, and ABRSH3 contributed to the recognition of a hypothetical, complementary binding motif within Asef2 using the GST fusion proteins of these regions (Fig. 4D) to precipitate Asef2. FLAG-tagged Asef2 expressed in cells precipitated with only the GST-ABRSH3 (Fig. 6C). The same was true of FLAG-tagged Asef1 that was precipitated with Asef1 GST fusion proteins. Similar results were obtained using recombinant, full-length Asef2 purified from Sf9 cells (Fig. 6D), indicating that the interaction

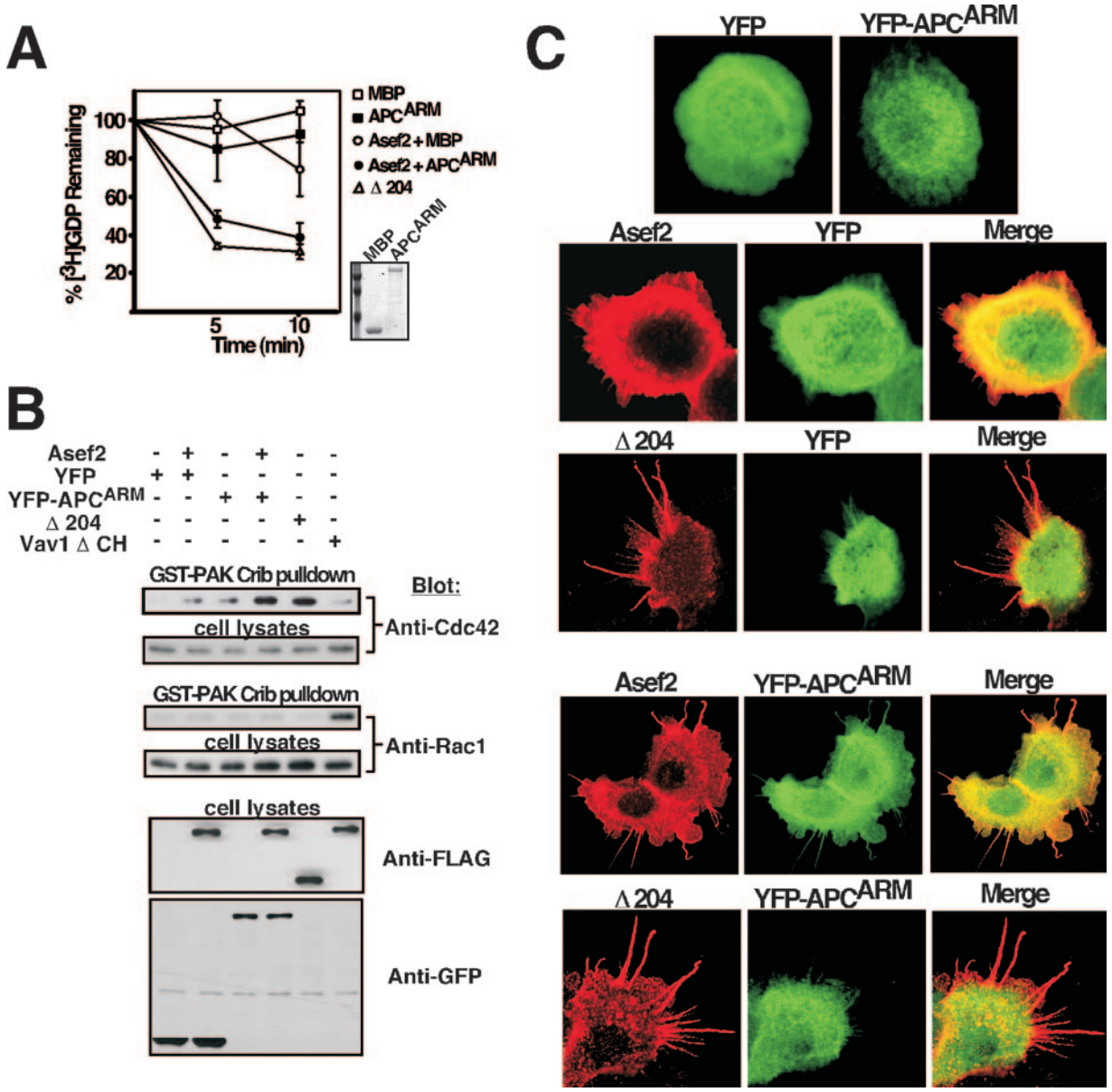

FIG. 5. The APC^{ARM} stimulates Asef2 GEF activity. (A) An in vitro exchange assay was performed using [^{3}H]GDP-loaded Cdc42 and the indicated Flag-His-tagged Asef2 and MBP fusion proteins. Either a buffer control or full-length Asef2 was incubated with an approximately equal-molar amount (30 nM) of MBP or an MBP fusion of the APC^{ARM} for 30 min prior to adding to the exchange assay. Insert indicates the purity of 1 μg MBP and MBP-APC^{ARM} applied to an SDS-PAGE gel and stained with Coomassie blue. (B) Lysates from HeLa cells coexpressing either YFP or YFP-tagged APC^{ARM} and a control vector or FLAG-tagged Asef2 were used in a PAK-CRIB pull-down assay. Rac1, Cdc42, and the FLAG-tagged Asef2 proteins were detected as described in the legend of Fig. 2, and YFP-tagged proteins were detected using an anti-GFP antibody. Cell lysates represent 10 μg of total protein. The blot reflects data from three independent experiments. (C) BxPc3 cells coexpressing YFP or the YFP-APC^{ARM} and either FLAG-tagged Asef2 or the Δ204 mutant were grown on coverslips for 24 h, fixed with paraformaldehyde, permeabilized, and stained using an anti-FLAG antibody and a tetramethyl rhodamine isothiocyanate anti-mouse secondary antibody. Cells expressing YFP or the YFP-APC^{ARM} are provided as negative controls. Images are representative of the transfected population.

was direct. Furthermore, when the GST fusion proteins of the ABR, SH3, and the ABRSH3 were coincubated with the Δ204 mutant of Asef2 in an exchange assay, only the ABRSH3 fully inhibited exchange activity (Fig. 6E). Taken together, these results indicate that the SH3 domain is required and sufficient for inhibiting Asef2, but the tandem arrangement of the ABRSH3 probably maximizes binding contacts within the protein. Furthermore, the GST-SH3 domain fusion protein did not inhibit the Δ204 mutant in *trans*, indicating that the independent SH3 domain can only inhibit Asef2 when the structure is provided in the proper intramolecular context, such as in the Δ140 mutant.

Although our experiments demonstrated the ABRSH3 inhibited the Δ204 mutant, it was unclear which region of the protein was providing the complementary binding site. In order to inhibit the Δ204 mutant, the ABRSH3 binding site

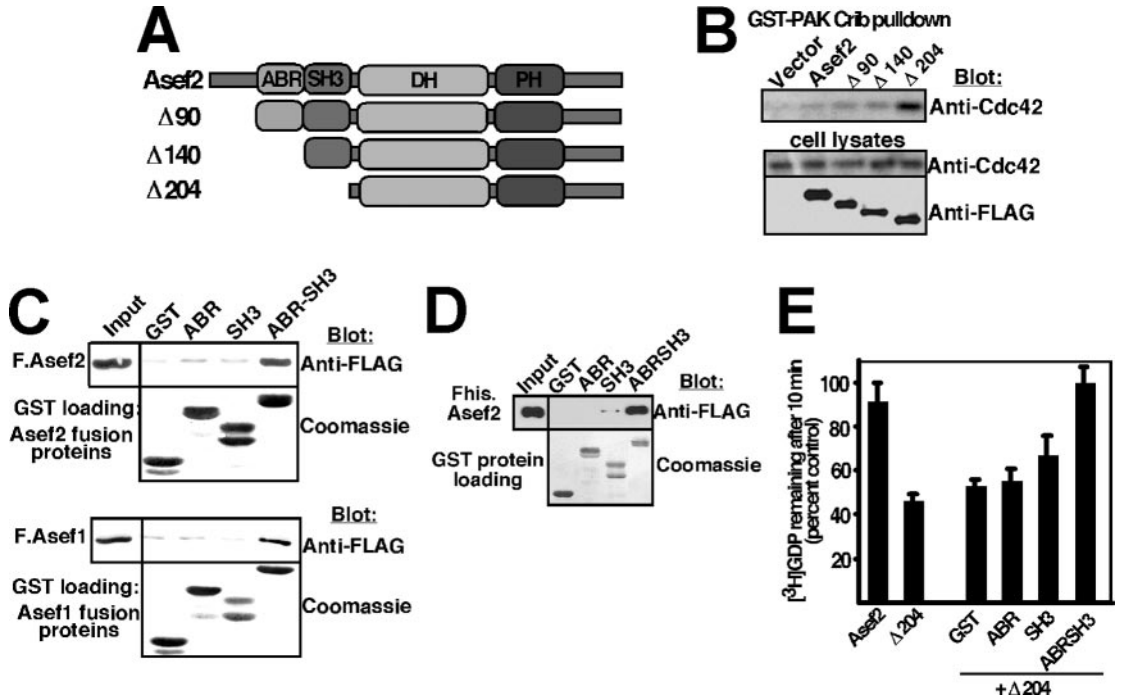

FIG. 6. The ABRSH3 inhibits Asef2. (A) A schematic representation of the N-terminal truncation mutants used in the experiment presented in panel B. Numbers indicate the first amino acid retained in the sequence of the truncation mutation. (B) HeLa cells expressing FLAG-tagged Asef2 and the Δ90, Δ140, and Δ204 mutants were used in a PAK-CRIB pull-down assay, and proteins were detected as described in the legend of Fig. 2. (C) Lysate from cells expressing FLAG-tagged Asef2 or Asef1 was incubated with the GST fusion proteins of the ABR, SH3, and ABRSH3 (Fig. 3D). Lysate from cells expressing Asef2 was incubated with Asef2 GST fusion proteins, and lysate from cells expressing Asef1 was incubated with Asef1 GST fusion proteins. Coomassie staining indicates the relative amount of the fusion proteins used in the experiment. (D) Flag-His-tagged Asef2 purified from Sf9 cells (0.25 μg) was used in a GST precipitation assay with the same fusion proteins indicated in panel C. (E) The Flag-His-tagged Δ204 mutant was incubated with a threefold molar excess (i.e., 75 nM) of either GST or GST fusions of the ABR, SH3, and ABRSH3 domains before being added to [^{3}H]GDP-loaded Cdc42. Aliquots were removed after 10 min of exchange, and the radioactivity was counted. The data points were normalized to a buffer control and represent the mean of triplicate samples ± standard deviation.

would have to lie within the DH-PH region, the last 91 amino acids lying just after the PH domain, or within a combination of the regions. To determine where the intramolecular association occurred, we generated a C-terminal deletion mutant that removed the last 91 amino acids from the tail of the protein (Δ561) and expressed it in cells along with full-length Asef2 and the Δ204 mutant. In coprecipitation assays, full-length Asef2 and the Δ204 mutant consistently bound to the GST-ABRSH3, while the Δ561 C-terminal truncation mutant failed to precipitate with the fusion protein (Fig. 7A). Furthermore, the Δ204 mutant always bound more tightly to the GST-ABRSH3 than the full-length protein, presumably because the Δ204 mutant lacks an intramolecular ABRSH3 that would otherwise compete with the GST-ABRSH3 for the complementary binding site. We confirmed direct binding of the ABRSH3 to the C-terminal tail using GST fusions of the C-terminal tail and the DH-PH and MBP fusions of the ABR, the SH3, and the ABRSH3 (Fig. 7B). All three MBP proteins interacted preferentially with the tail segment of the protein, demonstrating a role for both the ABR and SH3 domain in binding to the tail independently; however, the interaction was strongest with the tandem ABRSH3, again indicating that the tandem arrangement of the two regions provided the optimum interaction. Finally, in exchange assays, addition of an equal, stoichiometric amount of the tail segment activated full-length Asef2 to a level comparable to the Δ204 mutant, indicating in *trans* addition of a tail fusion protein released the ABRSH3 intramolecular tail interaction, opening Asef2 to an active conformation (Fig. 7C). These findings suggest that the tail region interacts with the Asef2 ABRSH3 in a manner analogous to the APC^{ARM} interaction, but it occurs in an intramolecular context, where the tail can inhibit the activity of the protein by blocking a region that is required for exchange activity.

The C-terminal tail contains an element that is required for Asef2 exchange activity. The model derived from our data indicates that the ABRSH3 inhibits Asef2 activity by binding the tail region of the protein. The obvious prediction is that deletion of the C-terminal tail should constitutively activate Asef2, similar to the Δ204 mutant. However, cells transfected with either a Δ561 or a Δ600 C-terminal deletion mutant (Fig. 8A) did not show any increase in the amount of active Cdc42 detected in precipitation assays (Fig. 8B). In order to ensure that our results were not due to an autoinhibitory factor that was not detected in our binding assays, a series of tail deletions was made in the context of the Δ204 mutation (Fig. 8A). In these assays, Asef2 GEF activity was eliminated with the deletion of the last 32 amino acids from the tail (residues 204 to 620) and diminished with deletion of the last 22 amino acids

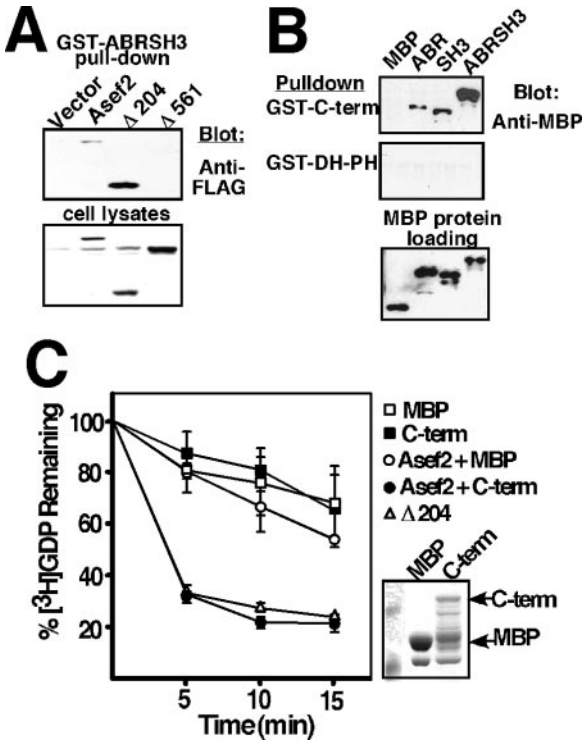

FIG. 7. The ABRSH3 binds to the C-terminal tail of Asef2. (A) HeLa cells expressing FLAG-tagged Asef2 and the Δ204 and Δ561 truncation mutants were used in a precipitation assay with the GST-ABRSH3 fusion protein. (B) MBP fusion proteins of the ABR, the SH3, and the ABRSH3 (1 μg of each protein) were incubated with GST fusion proteins of the C-terminal tail and the DH-PH domain of Asef2. Coprecipitating MBP proteins were detected with immunoblotting and anti-MBP antibody. (C) An MBP fusion protein of the Asef2 C-terminal tail (30 nM) was incubated with Flag-His-Asef2 and used in an in vitro exchange assay. The panel shows the relative purity of 1.5 μg of MBP and the C-terminal tail fusion protein used in the assay by SDS-PAGE and Coomassie staining. Typically, the C-terminal tail fusion protein did not purify as single band, and the concentration of the MBP-C-terminal tail fusion protein added to the assay represents the concentration of the upper, highest molecular weight band and was calculated by determining the fraction of protein that was present in this band (see Materials and Methods). Control MBP was added at a concentration comparable to the amount of total C-terminal tail protein added to the assay (i.e., about 300 nM). Points indicate the mean of triplicate samples and error bars represent the standard deviation.

(Fig. 8C, 204–630). These results were confirmed using in vitro exchange assays and proteins purified from Sf9 cells (data not shown). This led us to hypothesize that not only was the C-terminal tail involved in an intramolecular association with the ABRSH3, but also it might be involved in stimulating Asef2 GEF activity. Therefore, we used the MBP fusion protein of the C-terminal tail in an exchange assay to determine if it could rescue the defect detected with the mutant containing residues 204 to 620 (204–620 mutant). The fusion protein of the C-terminal tail restored activity of the inactive 204–620 mutant to nearly the same activity detected with the Δ204 mutant when the tail was provided at an equal-molar ratio (Fig. 8D and E). Additionally, the 204–620 mutant increased the amount of active Cdc42 detected in precipitation assays when it was co-expressed with an YFP-tagged fusion protein of the C-terminal

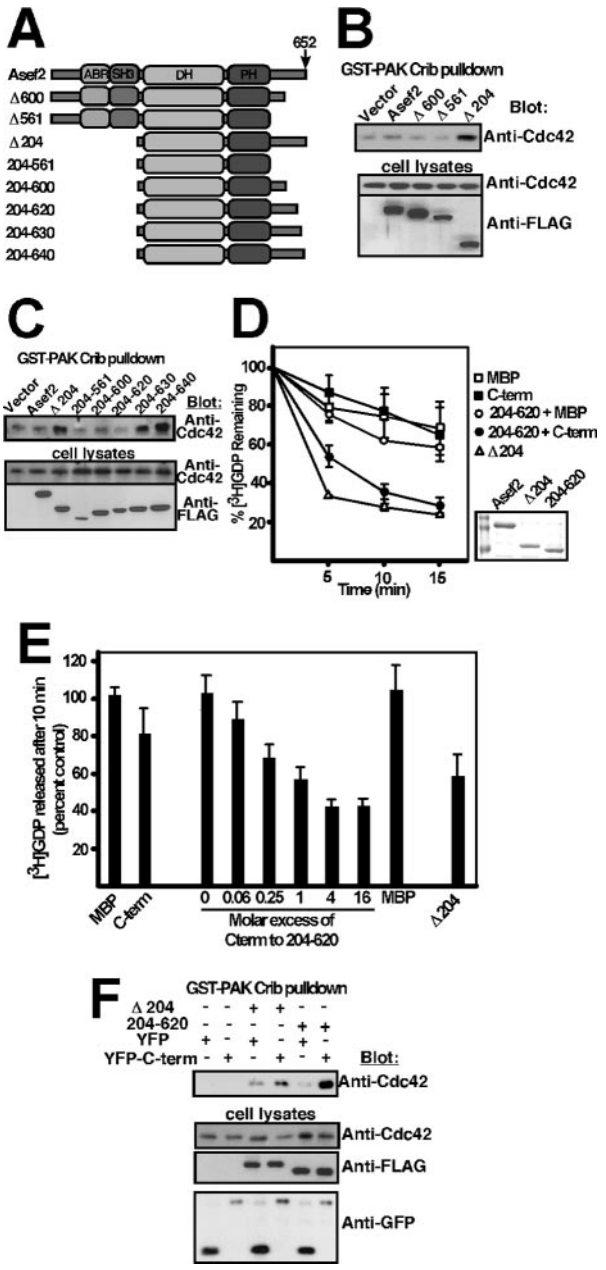

FIG. 8. The C-terminal tail of Asef2 is required for exchange activity. (A) Schematic of the truncation mutants generated to test the effect of the C-terminal tail on Asef2 autoinhibition and activation. (B and C) HeLa cells expressing the indicated FLAG-tagged Asef2 truncations were used in a PAK-CRIB pull-down assay and immunoblotted as described in the legend of Fig. 2. The blots reflect data from three independent experiments. (D) The 204–620 truncation mutant of Asef2 was used in an exchange assay with the C-terminal tail in a manner similar to that described in the legend to Fig. 7. (E) In a titration experiment, the C-terminal tail was provided at substoichiometric (0.06-fold) and near saturating concentrations (16-fold) in comparison to the concentration of the Asef2 204–620 mutant (25 nM). The amount of [^{3}H]GDP-labeled Cdc42 was determined after 10 min. The amount of MBP C-terminal tail added to the exchange assay was determined as described in the legend to Fig. 7. (F) The 204–620 mutant or the Δ204 truncation mutant was expressed in HeLa cells with either YFP or an YFP-tagged version of the C-terminal (C-term) tail. Lysates from the cells were used in a GST-PAK-CRIB pull-down assay to detect Cdc42 activation. The blot reflects data from two independent experiments.

tail (Fig. 8F). Together, these results clearly indicate that the tail positively regulates Asef2 activity.

DISCUSSION

The Asef family of Cdc42-specific GEFs. Our findings for Asef2 run counter to two key findings from the initial paper on Asef1. First, Asef1 and Asef2 are both Cdc42-specific exchange factors. While both Asef2 and Asef1 appear to affect cell migration, identifying Cdc42 as their GTPase substrate is a significant step forward toward defining their exact role in this process. It is notable that the Asef proteins appear to bind Rac1. Although we have not exhaustively pursued how Rac1 may regulate Asef2, we have not detected an effect on Cdc42 exchange when excess Rac1 is preincubated with Asef2 in in vitro exchange assays (data not shown). This suggests that Rac1 does not regulate Asef2 activity in a way that has been reported for Cool-2/α-Pix (14). Although Rac1 suppression did not have an effect on filopodial formation stimulated by the Δ204 mutant (Fig. 3B), it is possible that Rac1 is somehow important for localization of endogenous Asef2 in a manner that is reminiscent of Rac1 binding to the RhoA-specific GEF, Lfc (17).

Determining the substrate preference for Asef1 and Asef2 places these proteins upstream of events requiring activation of Cdc42, such as cellular polarization and spindle fiber stabilization (26). In fact, the Asef proteins may be required for the activation of Cdc42 detected in scratch-wounded cells and may in fact colocalize with APC at the plus-end of microtubules along the leading edge (10). It should be noted that APC localization has currently been placed downstream of Cdc42 and Par6/PKCζ activation (12), and it is possible that APC localization is initiated by a relatively small amount of active Cdc42 that is not due to stimulation of Asef1 or Asef2 by APC. Once APC is appropriately localized, the APC^{ARM} could be stimulated to interact with the Asef proteins, leading to a robust increase in Cdc42 activity at the front edge of the polarized cells, producing WASP-derived actin structures and activating PAK, resulting in βPIX accumulation near the leading edge (7).

Identifying Cdc42 as the GTPase substrate for Asef1 and Asef2 also places the two proteins in closer relation to collybistin, which was previously shown to activate Cdc42 (30). The result suggests that the three proteins are essentially a family of GEFs with similar structural and biochemical characteristics, although their cellular function is probably significantly different. Currently, two splice variants of collybistin, I and II, have been identified (23). Collybistin I sequence is shown in Fig. 1A, and like the Asef proteins, its sequence includes an N-terminal SH3 domain. Collybistin II lacks the sequence corresponding to the SH3 domain and also has a shorter, divergent C-terminal tail sequence. Collybistin I and II expression is neuronal specific, where they act in conjunction with gephyrin to produce γ-aminobutyric acid type A receptor and inhibitory glycine (Gly) receptor clustering in postsynaptic neurons. Gephyrin anchors these receptors to the cytoskeletal framework of the neuron, and it has been suggested that collybistin is required for efficient localization of the receptors to the postsynaptic membrane (19, 23). It is unlikely that the function of the Asef proteins will overlap those of collybistin, since both Asef1 and Asef2 mRNA transcripts are expressed in a wider variety of tissues (Fig. 1C). Moreover, APC clearly regulates both Asef proteins, and we have not detected an interaction between APC and collybistin (M. J. Hamann and D. D. Billadeau, unpublished observation).

The tandem ABRSH3 acts as an inhibitory module and APC recognition site. The second disparity between our results and those reported for Asef1 is that there is not a clear, independent regulatory function for the Asef2 ABR. Notably, the exact deletion used to constitutively activate Asef1 was not specified in the Asef1 studies, and it is possible the truncation removed part or the entire SH3 domain; therefore, the inhibitory role of the SH3 domain may have been overlooked (21, 22). In our experiments, both the ABR and the SH3 domain contribute to maintaining Asef2 in an inhibited conformation, with the SH3 domain playing a dominant role. SH3 domain interactions with specific polyproline ligands have been relatively well characterized, and in order to better understand the regulatory role of the SH3 domain, we have made mutations within the SH3 domain that are known to disrupt binding to both canonical and noncanonical SH3 motifs at the cleft region of the domain. Interestingly, these mutations have not activated Asef2, even when provided in the context of the Δ140 truncation mutant (M. J. Hamann and D. D. Billadeau, unpublished observations) and may indicate that the surface of the SH3 domain responsible for binding to the C-terminal tail may be significantly different than the cleft region that is typically involved in the recognition of polyproline sequences. This view is supported in the experiments that demonstrated binding to full-length Asef2, the MBP fusion protein of the tail, and inhibition of the Δ204 truncation mutant in exchange assays was only maximal when the tested protein was presented with the tandem arrangement of the ABRSH3. Using the individual pieces of either the ABR or the SH3 domain did little in these assays, demonstrating that the interaction with the C-terminal tail is complex and involves more than the ABR alone or a typical SH3 domain interaction.

In comparison to the autoinhibitory interaction of the C-terminal tail and the ABRSH3, binding of the APC^{ARM} to Asef2 localized primarily to the SH3 domain alone. It remains to be seen if the APC^{ARM} simply displaces the C-terminal tail from the ABRSH3 and activates Asef2 or if it binds to different portions of the SH3, resulting in an allosteric shift that displaces the C-terminal tail. Currently, we have not extensively tested how the Asef2 SH3 domain mutants affect binding to the APC^{ARM}. It is notable, however, that the APC^{ARM} does not contain obvious polyproline stretches, indicating that the interaction probably occurs through an atypical SH3 domain recognition motif. In fact, if the interaction between the APC^{ARM} and the SH3 domain occurs on a surface other than the polyproline binding surface, it is possible that APC may release the ABRSH3 region and facilitate both GEF activation and binding to a downstream effector protein through a canonical SH3-mediated interaction.

Interestingly, while collybistin I and II may share substrate specificity, it is not entirely clear whether these proteins are self-regulated through an autoinhibitory motif. It is known that the GEF activity of collybistin II is directly inhibited through its interaction with gephyrin (39). If binding to gephyrin is all that is required to inhibit collybistin I, the SH3 domain of this

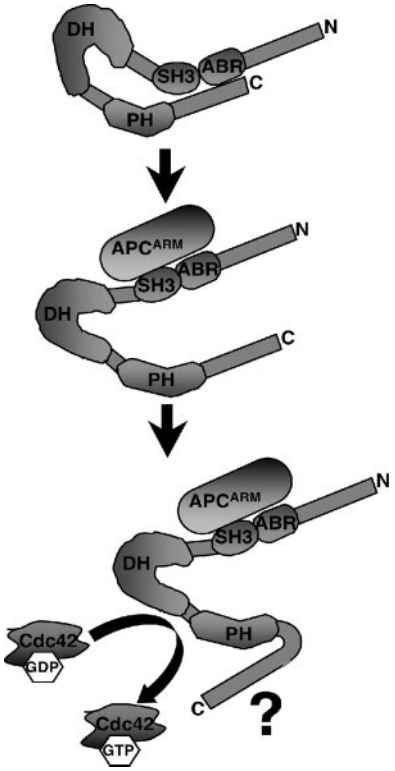

FIG. 9. A model of Asef2 regulation. Asef2 is normally in an inactive conformation until activated by APC. Stimulation by the APC^{ARM} releases the autoinhibitory ABRSH3 from the C-terminal tail of Asef2. Releasing the tail from Asef2 facilitates Cdc42 exchange, possibly by binding Cdc42 or activating the DH-PH region of the GEF.

variant may primarily function to localize the protein to the appropriate subcellular structures. If this is the case, the fact that collybistin does not contain an N-terminal sequence corresponding to the ABR may represent sequence divergence between the three proteins, since this region could be dispensable for collybistin's function.

The C-terminal tail auto-activation element. At this time, it is uncertain how the tail contributes to the exchange reaction; however, another Rho-GEF, Vav, has been shown to exchange more efficiently when additional C-terminal sequence beyond the DH-PH is included in the protein. The cysteine rich domain of Vav lies just beyond the canonical DH-PH region and enhances Rac1 exchange through a direct interaction with the small GTPase (20). Interestingly, a portion of collybistin's C-terminal tail has been suggested to form a coiled-coil structure (23), and it is possible that a similar structure in Asef2 creates a segment that is involved in GTPase recognition analogous to a short coiled-coil structure in Rho-associated kinase that participates in RhoA recognition (9). Currently, we have not been successful in precipitating Cdc42 with the C-terminal tail of Asef2 in initial pull-down experiments (data not shown), but it is possible that the C-terminal tail of Asef2 may directly recognize Cdc42 and facilitate its turnover. It is also possible that the tail somehow is facilitating protein dimerization in a manner analogous to α-Pix and that the tail-to-tail dimerization is somehow required for Asef2 exchange activity (14). Regardless of the specific mechanism, our data strongly indicate that the DH-PH region alone (i.e., Asef2 residues 204 to 561) will not rapidly catalyze Cdc42 exchange unless the tail is present. Conversely, it is also clear that the tail cannot function independently as a GEF, since the L259Q and W552L point mutants (Fig. 1F) successfully inactivate the exchange activity of the Δ204 mutant.

Together, our results describe a model (Fig. 9) where the tail of Asef2 binds the ABRSH3 to maintain the protein in an inhibited confirmation yet also requires the tail for optimal Cdc42 exchange. Accordingly, the role of the ABRSH3 may be simply to keep the C-terminal activation element from participating in the exchange reaction. In this case, the APC^{ARM} simply acts to displace the tail from the ABRSH3, resulting in rapid Cdc42 exchange. Future experiments will be aimed at deciphering the amino acid residues in the C-terminal tail that contribute to binding the ABRSH3 and which residues potentiate Asef2 activity and Cdc42 turnover, as well as determining how Asef2 becomes activated in migrating cells.

ACKNOWLEDGMENTS

We thank Kent Rossman and Channing Der for providing information on the Cdc42 specificity of Asef1.

This work was supported by the Mayo Foundation and NCI SPORE grant CA102701 to D.D.B.

REFERENCES

1. **Aghazadeh, B., W. E. Lowry, X. Y. Huang, and M. K. Rosen.** 2000. Structural basis for relief of autoinhibition of the Dbl homology domain of proto-oncogene Vav by tyrosine phosphorylation. Cell **102:**625–633.
2. **Benard, V., and G. M. Bokoch.** 2002. Assay of Cdc42, Rac, and Rho GTPase activation by affinity methods. Methods Enzymol. **345:**349–359.
3. **Bi, F., B. Debreceni, K. Zhu, B. Salani, A. Eva, and Y. Zheng.** 2001. Autoinhibition mechanism of proto-Dbl. Mol. Cell. Biol. **21:**1463–1474.
4. **Bienz, M.** 2002. The subcellular destinations of APC proteins. Nat Rev. Mol. Cell. Biol. **3:**328–338.
5. **Bourguignon, L. Y., H. Zhu, L. Shao, and Y. W. Chen.** 2000. Ankyrin-Tiam1 interaction promotes Rac1 signaling and metastatic breast tumor cell invasion and migration. J. Cell Biol. **150:**177–191.
6. **Burridge, K., and K. Wennerberg.** 2004. Rho and Rac take center stage. Cell **116:**167–179.
7. **Cau, J., and A. Hall.** 2005. Cdc42 controls the polarity of the actin and microtubule cytoskeletons through two distinct signal transduction pathways. J. Cell Sci. **118:**2579–2587.
8. **Dikovskaya, D., J. Zumbrunn, G. A. Penman, and I. S. Nathke.** 2001. The adenomatous polyposis coli protein: in the limelight out at the edge. Trends Cell Biol. **11:**378–384.
9. **Dvorsky, R., L. Blumenstein, I. R. Vetter, and M. R. Ahmadian.** 2004. Structural insights into the interaction of ROCKI with the switch regions of RhoA. J. Biol. Chem. **279:**7098–7104.
10. **Etienne-Manneville, S., and A. Hall.** 2003. Cdc42 regulates GSK-3β and adenomatous polyposis coli to control cell polarity. Nature **421:**753–756.
11. **Etienne-Manneville, S., and A. Hall.** 2002. Rho GTPases in cell biology. Nature **420:**629–635.
12. **Etienne-Manneville, S., J. B. Manneville, S. Nicholls, M. A. Ferenczi, and A. Hall.** 2005. Cdc42 and Par6-PKCzeta regulate the spatially localized association of Dlg1 and APC to control cell polarization. J. Cell Biol. **170:**895–901.
13. **Faux, M. C., J. L. Ross, C. Meeker, T. Johns, H. Ji, R. J. Simpson, M. J. Layton, and A. W. Burgess.** 2004. Restoration of full-length adenomatous polyposis coli (APC) protein in a colon cancer cell line enhances cell adhesion. J. Cell Sci. **117:**427–439.
14. **Feng, Q., D. Baird, and R. A. Cerione.** 2004. Novel regulatory mechanisms for the Dbl family guanine nucleotide exchange factor Cool-2/alpha-Pix. EMBO J. **23:**3492–3504.
15. **Fernandez-Zapico, M. E., N. C. Gonzalez-Paz, E. Weiss, D. N. Savoy, J. R. Molina, R. Fonseca, T. C. Smyrk, S. T. Chari, R. Urrutia, and D. D. Billadeau.** 2005. Ectopic expression of VAV1 reveals an unexpected role in pancreatic cancer tumorigenesis. Cancer Cell **7:**39–49.
16. **Fodde, R., R. Smits, and H. Clevers.** 2001. APC, signal transduction and genetic instability in colorectal cancer. Nat. Rev. Cancer **1:**55–67.
17. **Glaven, J. A., I. P. Whitehead, T. Nomanbhoy, R. Kay, and R. A. Cerione.** 1996. Lfc and Lsc oncoproteins represent two new guanine nucleotide exchange factors for the Rho GTP-binding protein. J. Biol. Chem. **271:**27374–27381.

18. **Gomez, T. S., M. J. Hamann, S. McCarney, D. N. Savoy, C. M. Lubking, M. P. Heldebrant, C. M. Labno, D. J. McKean, M. A. McNiven, J. K. Burkhardt, and D. D. Billadeau.** 2005. Dynamin 2 regulates T cell activation by controlling actin polymerization at the immunological synapse. Nat. Immunol. **6:**261–270.
19. **Grosskreutz, Y., A. Hermann, S. Kins, J. C. Fuhrmann, H. Betz, and M. Kneussel.** 2001. Identification of a gephyrin-binding motif in the GDP/GTP exchange factor collybistin. Biol. Chem. **382:**1455–1462.
20. **Heo, J., R. Thapar, and S. L. Campbell.** 2005. Recognition and activation of Rho GTPases by Vav1 and Vav2 guanine nucleotide exchange factors. Biochemistry **44:**6573–6585.
21. **Kawasaki, Y., R. Sato, and T. Akiyama.** 2003. Mutated APC and Asef are involved in the migration of colorectal tumour cells. Nat. Cell Biol. **5:**211–215.
22. **Kawasaki, Y., T. Senda, T. Ishidate, R. Koyama, T. Morishita, Y. Iwayama, O. Higuchi, and T. Akiyama.** 2000. Asef, a link between the tumor suppressor APC and G-protein signaling. Science **289:**1194–1197.
23. **Kins, S., H. Betz, and J. Kirsch.** 2000. Collybistin, a newly identified brain-specific GEF, induces submembrane clustering of gephyrin. Nat. Neurosci. **3:**22–29.
24. **Knaus, U. G., and G. M. Bokoch.** 1998. The p21Rac/Cdc42-activated kinases (PAKs). Int. J. Biochem. Cell. Biol. **30:**857–862.
25. **Lozano, E., M. Betson, and V. M. Braga.** 2003. Tumor progression: Small GTPases and loss of cell-cell adhesion. Bioessays **25:**452–463.
26. **Ma, C., H. A. Benink, D. Cheng, V. Montplaisir, L. Wang, Y. Xi, P. P. Zheng, W. M. Bement, and X. J. Liu.** 2006. Cdc42 activation couples spindle positioning to first polar body formation in oocyte maturation. Curr. Biol. **16:**214–220.
27. **Mosteller, R., J. Han, B. Das, and D. Broek.** 2000. Biochemical analysis of regulation of Vav, a guanine-nucleotide exchange factor for Rho family of GTPases. Methods Enzymol. **325:**38–51.
28. **Movilla, N., M. Dosil, Y. Zheng, and X. R. Bustelo.** 2001. How Vav proteins discriminate the GTPases Rac1 and RhoA from Cdc42. Oncogene **20:**8057–8065.
29. **Nolz, J. C., T. S. Gomez, P. Zhu, S. Li, R. B. Medeiros, Y. Shimizu, J. K. Burkhardt, B. D. Freedman, and D. D. Billadeau.** 2006. The WAVE2 complex regulates actin cytoskeletal reorganization and CRAC-mediated calcium entry during T cell activation. Curr. Biol. **16:**24–34.
30. **Reid, T., A. Bathoorn, M. R. Ahmadian, and J. G. Collard.** 1999. Identification and characterization of hPEM-2, a guanine nucleotide exchange factor specific for Cdc42. J. Biol. Chem. **274:**33587–33593.
31. **Ridley, A. J., and A. Hall.** 1992. The small GTP-binding protein Rho regulates the assembly of focal adhesions and actin stress fibers in response to growth factors. Cell **70:**389–399.
32. **Ridley, A. J., H. F. Paterson, C. L. Johnston, D. Diekmann, and A. Hall.** 1992. The small GTP-binding protein Rac regulates growth factor-induced membrane ruffling. Cell **70:**401–410.
33. **Riento, K., and A. J. Ridley.** 2003. Rocks: multifunctional kinases in cell behaviour. Nat. Rev. Mol. Cell. Biol. **4:**446–456.
34. **Rossman, K. L., C. J. Der, and J. Sondek.** 2005. GEF means go: turning on RHO GTPases with guanine nucleotide-exchange factors. Nat. Rev. Mol. Cell. Biol. **6:**167–180.
35. **Sahai, E., T. Ishizaki, S. Narumiya, and R. Treisman.** 1999. Transformation mediated by RhoA requires activity of ROCK kinases. Curr. Biol. **9:**136–145.
36. **Schiller, M. R., K. Chakrabarti, G. F. King, N. I. Schiller, B. A. Eipper, and M. W. Maciejewski.** 2006. Regulation of RhoGEF activity by intramolecular and intermolecular SH3 domain interactions. J. Biol. Chem. **281:**18774–18786.
37. **Self, A. J., and A. Hall.** 1995. Purification of recombinant Rho/Rac/G25K from *Escherichia coli*. Methods Enzymol. **256:**3–10.
38. **Sterpetti, P., A. A. Hack, M. P. Bashar, B. Park, S. D. Cheng, J. H. Knoll, T. Urano, L. A. Feig, and D. Toksoz.** 1999. Activation of the Lbc Rho exchange factor proto-oncogene by truncation of an extended C terminus that regulates transformation and targeting. Mol. Cell. Biol. **19:**1334–1345.
39. **Xiang, S., E. Y. Kim, J. J. Connelly, N. Nassar, J. Kirsch, J. Winking, G. Schwarz, and H. Schindelin.** 2006. The crystal structure of Cdc42 in complex with collybistin II, a gephyrin-interacting guanine nucleotide exchange factor. J. Mol. Biol. **359:**35–46.
40. **Yaku, H., T. Sasaki, and Y. Takai.** 1994. The Dbl oncogene product as a GDP/GTP exchange protein for the Rho family: its properties in comparison with those of Smg GDS. Biochem. Biophys. Res. Commun. **198:**811–817.
41. **Zheng, Y., D. J. Fischer, M. F. Santos, G. Tigyi, N. G. Pasteris, J. L. Gorski, and Y. Xu.** 1996. The faciogenital dysplasia gene product FGD1 functions as a Cdc42Hs-specific guanine-nucleotide exchange factor. J. Biol. Chem. **271:**33169–33172.